JOURNAL OF COMPUTATIONAL PHYSICS 10, 224–231 (1972)

Numerical Laplace Transform Inversion of a Function Arising in Viscoelasticity

I. M. LONGMAN

Department of Environmental Sciences, Tel-Aviv University, Israel

Received September 8, 1971

Tables and graphs are given of the inverse Laplace transform of a function appearing frequently in the operational solution of pulse propagation problems arising in viscoelasticity. The method of calculation is based on the inversion of elements of the Padé table of the function. This is made practical by use of a recursive method of constructing the Padé table due to the author.

I. INTRODUCTION

As early as 1931 in a paper entitled "Damping of Bodily Seismic Waves" Jeffreys [1] is led to consider the Laplace transform inversion of the function

$$\bar{f}(p) = (1/p)\exp\{-px/c(1+\tau p)^{1/2}\}. \tag{1}$$

Here p denotes the Laplace transform operator, and $\bar{f}(p)$ is related to its inverse $f(t)$ by the usual equation

$$\bar{f}(p) = \int_0^\infty e^{-pt} f(t)\,dt, \tag{2}$$

t denoting the time. Here in the usual equation of transmission of distortional waves in one dimension

$$\partial^2 v/\partial t^2 = (\mu/\rho)(\partial^2 v/\partial x^2), \tag{3}$$

where v is the (small, transverse) displacement, μ is a Lamé elastic constant, ρ is the density and x denotes distance, Jeffreys allows for imperfection of elasticity of the nature of elastic afterworking or firmoviscosity by replacing μ by

$$\mu\left(1+\tau\frac{\partial}{\partial t}\right), \tag{4}$$

where τ is a constant measured as a time. Writing c^2 for μ/ρ Equation (3) then becomes

$$\frac{\partial^2 v}{\partial t^2} = c^2\left(1+\tau\frac{\partial}{\partial t}\right)\frac{\partial^2 v}{\partial x^2}. \tag{5}$$

For a medium originally undisturbed we have, in operational form, the subsidary equation

$$\frac{\partial^2 \bar{v}}{\partial x^2} = \frac{p^2}{c^2(1 + \tau p)} \bar{v} \tag{6}$$

having the solution

$$\bar{v} = \bar{v}_0 \exp\{-px/c(1 + \tau p)^{1/2}\}, \tag{7}$$

on the assumption that the operational solution does not tend to infinity as $x \to \infty$. $\bar{v}_0$ is the (transformed) displacement at $x = 0$. If we assume that $v_0(t) = H(t)$ (the Heaviside unit function) so that v_0 is zero up to time 0 and unity afterwards, we have

$$\bar{v} = (1/p) \exp\{-px/c(1 + \tau p)^{1/2}\}. \tag{8}$$

This operational solution is of the form (1) which may therefore be regarded as representing the propagation of a transverse displacement in a bar placed along the x-axis caused by a unit step function displacement at time $t = 0$ at the end $x = 0$.

Essentially the same function (1) is obtained by Collins [2] in the problem of impulsive stress propagation in a Voigt solid. Collins uses a method of inversion involving parabolic cylinder functions of negative integral order, and is faced with convergence difficulties, since his expansion only converges well for large p.

Later Clark and Rupert [3] obtained various integral representations for the inverse of (1), and Jaramillo and Colvin [4] solve a similar problem using again the parabolic cylinder functions as suggested by Collins, and again only obtain accurate results for small t.

All these variations on the inversion of (1) suffer from considerable analytic complication and various types of convergence difficulties. In the present paper simple tables and graphs are presented for the inversion of (1). These have been obtained by the use of a rational approximation technique developed by the author [5]. In examining these solutions it is helpful to bear in mind the physical problem suggested by Jeffreys which is described above in Eqs. (3)–(8).

II. Theory and Computations

As a first step in the treatment of (1) we replace the two parameters x/c and τ by a single parameter σ in the following way. Writing $x/c = a$ (1) takes the form

$$\bar{f}(p) = a(1/ap) \exp\{-ap/(1 + \sigma ap)^{1/2}\} \tag{9}$$

where we have written $\sigma = \tau/a = c\tau/x$, a dimensionless parameter. We see now that it is sufficient to invert

$$\bar{g}(p) = (1/p)\exp\{-p/(1 + \sigma p)^{1/2}\} \tag{10}$$

and then by the similarity rule for Laplace transforms the inverse $f(t)$ of $\bar{f}(p)$ is

$$f(t) = g(t/a) = g(ct/x). \tag{11}$$

For the rest of this paper we consider the inversion of (10) for various values of σ on the understanding that the time variable t in the answer is really to be replaced by the dimensionless ct/x.

Two limiting cases immediately present themselves. If we take $\sigma = 0$ we have ordinary elasticity in the Jeffreys problem, and the inversion of (10) is immediate, yielding

$$g(t) = H(t - 1), \tag{12}$$

which we interpret as

$$f(t) = H((ct/x) - 1); \tag{13}$$

the unit step arrives at time x/c corresponding to the velocity c. Thus for small σ we expect $g(t)$ to approach the function $H(t - 1)$. We also have a useful analytical approximation when σ is large, using the fact that an approximation to $\bar{g}(p)$ valid for large p yields on inversion an approximation to $g(t)$ valid for small t.[1] If p is sufficiently large we have

$$\bar{g}(p) \doteq g_1(p) = 1/p\exp\{-(p/\sigma)^{1/2}\} \tag{14}$$

neglecting 1 compared with σp in the square root. The exact inverse of $g_1(p)$ is

$$g_1(t) = 1 - \operatorname{erf}\{\tfrac{1}{2}(\sigma t)^{-1/2}\} = \operatorname{erfc}[\tfrac{1}{2}(\sigma t)^{-1/2}], \tag{15}$$

where erf denotes the error function defined according to

$$\operatorname{erf} z = (2/\pi^{1/2})\int_0^z e^{-u^2}\,du. \tag{16}$$

Thus we have at the outset two limiting forms for our inverse as $\sigma \to 0$ and as $\sigma \to \infty$. The method of numerical inversion of $\bar{g}(p)$ adopted in this paper is based on the Padé table for the Taylor series expansion of $p\bar{g}(p)$ about the point $p = 0$. The work is facilitated by use of a recursive method developed by the author [5] for computation of the Padé table.

[1] The intention here is that if σ is large, $\sigma p > p$ and so for p large we can neglect 1 compared to σp in Eq. (10).

The next step, then, is the Maclaurin expansion of $p\bar{g}(p)$. By elementary methods we find the formal expansion

$$p\bar{g}(p) = \exp\{-p/(1+\sigma p)^{1/2}\} = \sum_{k=0}^{\infty} c_k p^k , \tag{17}$$

where

$$c_0 = 1, \qquad c_1 = -1, \qquad c_2 = (1+\sigma)/2,$$

and

$$c_k = (-1)^k \left\{ \frac{1}{k!} + \frac{\sigma/2}{(k-2)!} + \sum_{r=2}^{k-1} \frac{(k-r+2)(k-r+4)\cdots(k+r-2)}{(k-r-1)!\,r!} \left(\frac{\sigma}{2}\right)^r \right\}, \quad k > 2. \tag{18}$$

Of course if $\sigma = 0$, $p\bar{g}(p) = e^{-p}$ giving Eq. (12) on inversion.

For various values of σ the Padé table was constructed, and the diagonal elements divided by p and inverted, the whole process being carried out automatically in the computer. The procedure was to invert successive diagonal elements and establish the accuracy by comparing results. For example in Table I below a few of the results for the case $\sigma = 0.1$ are given. The elements in question are those on the leading diagonal of the Padé table, and they represent alternate convergents of the corresponding continued fraction to the power series (17).

TABLE I

Inversion of successive diagonal elements (divided by p) for the case $\sigma = 0.1$[a]

t	$N=2$	$N=3$	$N=4$	$N=5$	$N=6$	$N=7$	$N=8$
0	−0.8182	0.5437	−0.2887	0.1887	−0.0356	0.0067	−0.0004
0.5	0.2675	−0.0284	−0.0271	0.0186	0.0286	0.0277	0.0274
1.0	0.7049	0.6094	0.5666	0.5516	0.5480	0.5475	0.5475
1.5	0.8811	0.9070	0.9232	0.9280	0.9289	0.9290	0.9290
2.0	0.9521	0.9873	0.9945	0.9945	0.9944	0.9944	0.9944
2.5	0.9807	1.0008	1.0002	0.9997	0.9997	0.9997	0.9997

[a] N is the position of the element on the leading diagonal of the Padé table.

It is evident that as we proceed to the right in this table we have rapid convergence to a fixed inverse, except for small values of t for which, however, we will see that sufficient accuracy is given by $g_1(t)$ (Eq. (15)).

In the following two tables the "converged" values are tabulated for $t = 0$ (0.1) 2.6 and $\sigma = 0$ (0.1) 0.9, 1.1, 2.0. Approximate values were also obtained for $\sigma = .03, 05, 5.0$ and 10.0 but are not tabulated here. They are, however, represented graphically in the figures. For the smaller values of t for which four-figure accuracy

has not been achieved by the inversion of the rational function standing in the eight position on the Padé table diagonal (divided by p) the results are given in brackets and derive from this eighth position. Of course the exact value for $t = 0$ is always zero.

TABLE II

"Converged" values of $g(t)$ for $\sigma = 0.1(0.1)\,0.5$

t	$\sigma = 0.1$	$\sigma = 0.2$	$\sigma = 0.3$	$\sigma = 0.4$	$\sigma = 0.5$
0	(−0.0004)	(−0.0006)	(0.0012)	(−0.0022)	(−0.0038)
0.1	(−0.0001)	(−0.0001)	(0.0002)	0.0001	0.0013
0.2	(0.0000)	0.0009	(0.0065)	0.0181	0.0340
0.3	(0.0004)	0.0113	0.0365	0.0678	0.0998
0.4	0.0055	0.0437	0.0927	0.1389	0.1798
0.5	0.0274	0.1022	0.1676	0.2200	0.2627
0.6	0.0800	0.1828	0.2526	0.3036	0.3431
0.7	0.1685	0.2773	0.3409	0.3850	0.4186
0.8	0.2860	0.3774	0.4272	0.4616	0.4879
0.9	0.4175	0.4757	0.5085	0.5320	0.5507
1.0	0.5475	0.5674	0.5828	0.5957	0.6071
1.1	0.6638	0.6493	0.6490	0.6525	0.6574
1.2	0.7602	0.7201	0.7072	0.7027	0.7020
1.3	0.8351	0.7798	0.7574	0.7467	0.7414
1.4	0.8902	0.8288	0.8003	0.7849	0.7760
1.5	0.9290	0.8685	0.8366	0.8179	0.8063
1.6	0.9553	0.8999	0.8669	0.8463	0.8328
1.7	0.9725	0.9245	0.8922	0.8707	0.8559
1.8	0.9835	0.9436	0.9130	0.8914	0.8759
1.9	0.9903	0.9581	0.9301	0.9090	0.8933
2.0	0.9944	0.9691	0.9440	0.9239	0.9084
2.1	0.9968	0.9774	0.9553	0.9365	0.9214
2.2	0.9982	0.9836	0.9644	0.9471	0.9327
2.3	0.9990	0.9881	0.9718	0.9560	0.9424
2.4	0.9995	0.9914	0.9777	0.9635	0.9507
2.5	0.9997	0.9939	0.9824	0.9697	0.9579
2.6	0.9998	0.9956	0.9861	0.9749	0.9641

It may be remarked that the value $\sigma = 1$ is omitted from Table III. The reason is that for this value of σ the Taylor series (15) ceases to be normal and does not have a normal Padé table, and our method of computation [5] is not valid in this case. For the definition of normality of a power series and its Padé table the reader is referred to Perron [6].

TABLE III

"Converged" values of $g(t)$ for $\sigma = 0.6(0.1)\ 0.9,\ 1.1,\ 2.0$

t	$\sigma = 0.6$	$\sigma = 0.7$	$\sigma = 0.8$	$\sigma = 0.9$	$\sigma = 1.1$	$\sigma = 2.0$
0	(−0.0122)	(0.0148)	(0.0073)	(0.0128)	(0.0165)	(−0.0690)
0.1	(0.0033)	(0.0065)	(0.0142)	0.0206	(0.0360)	0.1334
0.2	(0.0523)	0.0730	0.0916	0.1113	0.1482	0.2780
0.3	0.1307	0.1597	0.1856	0.2101	0.2538	0.3841
0.4	0.2156	0.2470	0.2749	0.2997	0.3425	0.4641
0.5	0.2983	0.3284	0.3548	0.3778	0.4167	0.5263
0.6	0.3753	0.4021	0.4255	0.4457	0.4796	0.5760
0.7	0.4456	0.4683	0.4878	0.5049	0.5335	0.6167
0.8	0.5092	0.5273	0.5429	0.5568	0.5804	0.6509
0.9	0.5663	0.5799	0.5918	0.6026	0.6214	0.6801
1.0	0.6173	0.6267	0.6353	0.6432	0.6576	0.7056
1.1	0.6628	0.6684	0.6739	0.6793	0.6897	0.7280
1.2	0.7032	0.7055	0.7083	0.7115	0.7184	0.7480
1.3	0.7391	0.7385	0.7391	0.7403	0.7440	0.7659
1.4	0.7708	0.7679	0.7665	0.7661	0.7671	0.7821
1.5	0.7988	0.7940	0.7910	0.7892	0.7879	0.7969
1.6	0.8236	0.8173	0.8129	0.8099	0.8067	0.8103
1.7	0.8454	0.8379	0.8325	0.8285	0.8237	0.8226
1.8	0.8647	0.8563	0.8500	0.8453	0.8391	0.8340
1.9	0.8816	0.8726	0.8657	0.8604	0.8530	0.8444
2.0	0.8964	0.8871	0.8798	0.8740	0.8657	0.8541
2.1	0.9095	0.9000	0.8924	0.8862	0.8772	0.8630
2.2	0.9209	0.9114	0.9036	0.8973	0.8877	0.8713
2.3	0.9310	0.9215	0.9137	0.9072	0.8973	0.8790
2.4	0.9398	0.9305	0.9227	0.9162	0.9060	0.8862
2.5	0.9475	0.9385	0.9308	0.9243	0.9140	0.8928
2.6	0.9542	0.9456	0.9381	0.9316	0.9213	0.8991

Figure 1 shows a plot of $g(t)$ for various values of σ, and for comparison the step function $H(t - 1)$ corresponding to the case $\sigma = 0$ is also shown.

In order to show the manner in which $g(t)$ approaches $g_1(t)$ as σ increases, the results have been plotted as functions of σt in Fig. 2, where also $g_1(t)$ is plotted. It was convenient to use a logarithmic scale in the σt direction in order to include the full range of σt for which results were calculated, and yet to show clearly the shape of the initial part of the $g_1(t)$ curve. It is evident in Fig. 2 how the shapes of the curves vary continuously from that of $H(\sigma t)$ for $\sigma = 0$ to

$$g_1(t) = 1 - \operatorname{erf}\{\tfrac{1}{2}(\sigma t)^{-1/2}\}$$

as $\sigma \to \infty$. Also we see to what extent $g_1(t)$ gives a good approximation to $g(t)$ for small values of t.

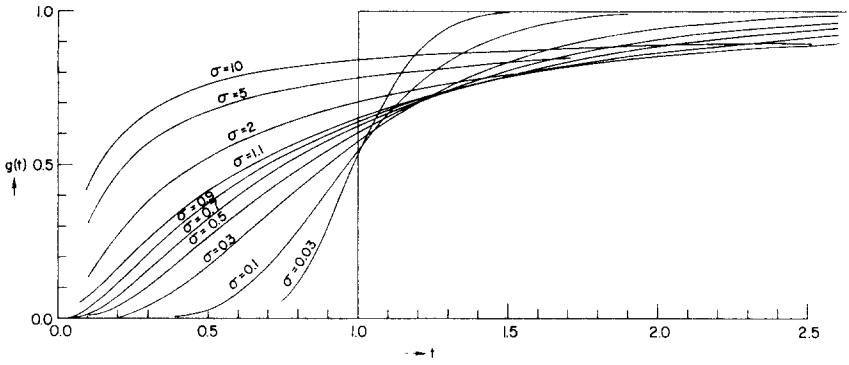

FIG. 1. The inverse $g(t)$ of $\bar{g}(p)$ [see Eq. (10)] is plotted for various values of σ. The step function $H(t-1)$ corresponds to the case $\sigma = 0$.

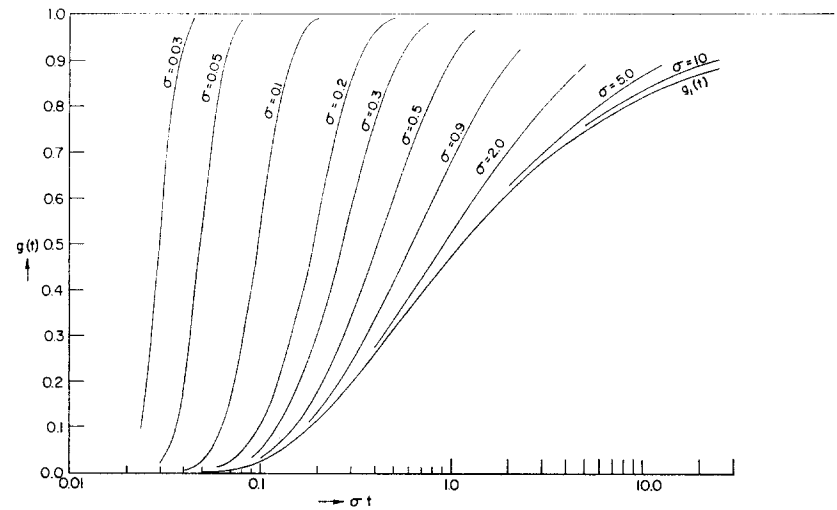

FIG. 2. The inverse $g(t)$ of $\bar{g}(p)$ [see Eq. (10)] is plotted against σt for various values of σ, using a logarithmic σt scale. For comparison the function $g(t)$ [Eq. (15)] is also shown, and corresponds to $\sigma \to \infty$. The unit function $H(\sigma t)$ corresponds to the case $\sigma \to 0$.

III. CONCLUSION

Numerical Laplace transform inversion has been achieved for an important problem in viscoelastic pulse propagation, and the results shown in tabular form and graphically.

ACKNOWLEDGMENTS

The attention of the author was drawn to this problem by J. Aboudi. The computations were carried out on the CDC 6600 computer at the Computation Centre of Tel-Aviv University.

REFERENCES

1. H. JEFFREYS, Damping in bodily seismic waves, *Mon. Not. Roy. Astr. Soc. Geophys. Supp.* **2** (1931), 318–323.
2. F. COLLINS, Plane compressional Voigt waves, *Geophys.* **35** (1960), 483–504.
3. G. B. CLARK AND G. B. RUPERT, Plane and spherical waves in a Voigt medium, *J. Geophys. Res.* **71** (1966), 2047–2053.
4. E. E. JARAMILLO AND J. D. COLVIN, *Transient waves in a Voigt medium, J. Geophys, Res.* **75** (1970), 5767–5773.
5. I. M. LONGMAN, Computation of the Padé table, *Int. J. Computer Math.* **B3** (1971), 53–64.
6. D. PERRON, "Die Lehre von dem Kettenbrüchen," p. 429, Chelsea, New York, 1950.